*33rd EPS Conference on Plasma Phys. Rome, 19 - 23 June 2006 ECA Vol.**30I**, P-1.137 (2006)*

First results from the new diagnostic neutral beam injector and charge-exchange diagnostic system on the TJ-II stellarator

J. M. Carmona, K. J. McCarthy, R. Balbín

Laboratorio Nacional de Fusión, Asociación EURATOM-CIEMAT, E-28040 Madrid, Spain

Introduction

The TJ-II is a 4-period, low magnetic shear, stellarator device with average minor radius ≤0.22 m and major radius of 1.5 m whose magnetic configurations are created by a system of external field coils [1]. It is designed to explore a wide range of rotational transforms ($0.9 \le \iota(0)/2\pi \le 2.2$) in low shear configurations ($\Delta q/q < -6\%$ in vacuum). To date, central electron densities and temperatures up to 1.7×10^{19} m^{-3} and 2 keV respectively have been achieved in plasmas created and maintained by electron cyclotron resonance heating (f=53.2 GHz tuned to 2nd harmonic, $P_{ECRH} \le 600$ kW, X-mode polarization). Recently, operation has commenced on one of two neutral beam injectors (NBI) each of which will produce ≤300 ms pulses of neutral hydrogen accelerated to ≤40 keV to provide up to 1.2 MW of additional heating.

During the spring 2006 campaign a diagnostic neutral beam injector (DNBI) and a charge-exchange recombination spectroscopy (CXRS) diagnostic were commissioned on the TJ-II. This compact DNBI provides 5 ms long pulses, two per discharge, of neutral hydrogen accelerated to 30 keV and with equivalent current of 3.3 equ. A [2]. See Table 1. In parallel, a dedicated bidirectional (two vertical opposing views) multi-channel spectroscopic diagnostic was designed and assembled to measure poloidal Doppler shifts and widths with ≤1 cm separation between sightlines. It incorporates two 12-channel fiber arrays, an f/1.8 holographic transmission-grating based spectrograph (centred at 529 nm), plus a back-illuminated CCD camera. Finally, a flexible coupling to the TJ-II permits the DNBI to follow the plasma centre when varying the magnetic configuration (*i.e.*, plasma size, centre, and radius all vary).

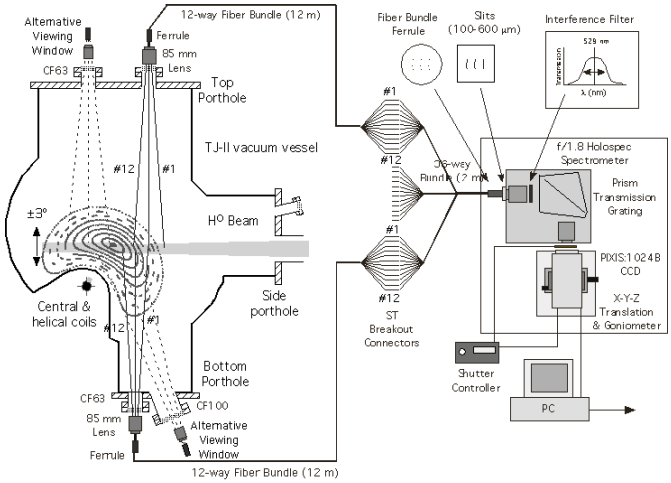

Fig. 1: Cross-sectional view of the TJ-II vacuum chamber and the DNBI.

Here, after outlining the new diagnostic, we present and discuss the first active experimental results obtained with it. In the first instance, these results highlight the capabilities and limitations of the actual system while also providing guidelines for future upgrades, for instance, boronized vacuum wall conditions in TJ-II diminish impurity line emission strength due to reduced impurity content. In the second instance, these preliminary results provide a first quantitative/qualitative evaluation of ion temperature and velocity of completely ionized impurities in the hot TJ-II plasma centre.

Ion source type	Arc source
Beam energy	10 to 30 keV
Extracted ion current	≤4 A
Focal length	170 cm
1/e divergence	≤0.7 degree
1/e radius at focus	~2.1 cm
(H, H_2, H_3)	~90%, ~8%, ~2%
Pulse length	≤5 ms
Pulses per discharge	2
Delay between pulses	≥50 ms

Table 1

The CXRS Diagnostic

The TJ-II possesses a complicated vacuum-vessel geometry, a bean-shaped plasma cross-section, and a fully 3-dimensional plasma structure. Fortuitously, top and bottom viewports, with direct sightlines across almost the complete plasma-beam interaction column, were available in the DNBI sector (A7). As opposing views provide a precise relative wavelength calibration, precise knowledge of the central wavelength of an emission line is not essential. Also, optical access (although indirect) is available from a nearby tangential viewing port for making toroidal measurements, but at present only poloidal components have been installed. Nonetheless, the possibility to incorporate toroidal viewing optics has been contemplated.

For poloidal measurements, a set of collection optics was installed in the top and bottom vacuum ports of sector A7. See Fig. 1. Each consists of fused quartz window/internal shutter assembly, a commercial camera lens and a fiber optic bundle. At each lens focus, twelve fibers are pitched in a single linear array, with 1 mm separation between centers. Note, the magnification of the fibers at the beam location is ~9. At the other end the bundles are connected to a single long 36-fiber bundle that terminates in a ferrule fixed to the spectrometer input. The remaining 12 fibers of the 36-way bundle are designated for toroidal viewing. At the spectrometer input the 36 fibers are permanently stacked into three curved arrays of 12 fibers, with 1 and 5 mm separations between fiber centers and arrays

respectively. Curved arrays are needed to compensate for the strong curvature in the image plane of short focal length spectrometer employed [3].

The light dispersion element is a Holospec spectrometer with a transmission grating sandwiched between two BK7 prisms, now commonly used for fusion plasma spectroscopy [4]. This set-up selected results in a magnification of ~1 and a focal-plane dispersion of 11.5 Å/mm on-axis for the C VI emission line at 5290 Å, n = 8 – 7. In addition, a bandpass filter centered on 5290 Å prevents spectral overlapping at the image plane of light from the multiple fiber arrays. Finally, interchangeable entrance slits (100 & 200 μm) permit the system to be optimized for narrow instrument function or for higher photon throughput.

A fast high-efficiency back-illuminated CCD camera is situated at the imaging plane. Its 13.3 x 13.3 mm active area is large enough to collect spectra from the 3 arrays. Also, a very fast thin mechanical shutter (≥4.5 ms time window) prevents illumination during CCD readout. With on-chip binning, 12 spectra can be readout time between the DNBI pulses (≥50 ms) so multiple frames can be collected during TJ-II discharges (≤300 ms).

Fiber alignment in the vertical plane of the TJ-II vacuum vessel was performed by illuminating the fiber bundle with a bright light source and observing, through an unused viewport, the orientation and location of the resultant bright spots with respect to markings on the inside of the opposing vacuum flange. In this way, the sightlines through plasmas can be determined using a cross-sectional machine drawing and magnetic configuration maps. Instrument set-up and checkout, as well as wavelength calibration and instrument function determination, were performed using pen type Ne and Xe lamps. From this, the wavelength dispersion at the detector center was found to be 11.5 Å/mm with +/- 7% variation at +/- 5 mm. Also, with 100 μm slits the instrument function was ~12.3 pixels (~1.84 Å) at the focal plane center while at 5 mm away it was ~8.5 pixels (1.36 Å).

First results

Once aligned and checked the calibrated system was used to determine C VI temperatures in a low-density TJ-II plasma, i.e. $\tilde{n}_e$ = 4.5 x 10^{18} m^{-3}. See Fig. 2. Impurity temperatures around 165 ± 15 eV were obtained for central lines of

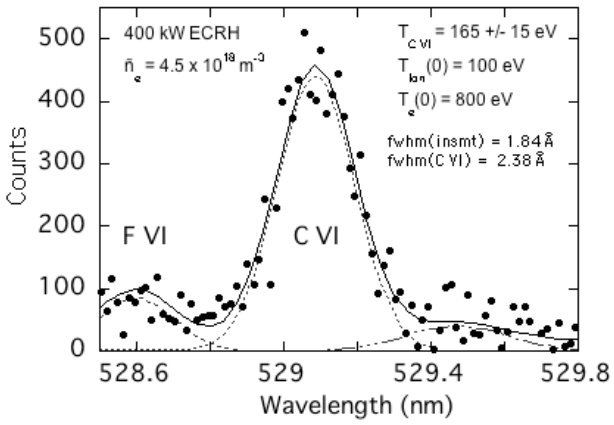

Fig. 2. Impurity ion temperature obtained by shot to shot technique.

sight. This is somewhat higher than the majority ion temperature measured for the same discharge using the nearby passive NPA diagnostic [5], *i.e.* 100 eV. However, anomalous impurity temperatures, attributed to non-thermal velocities, have been reported previously in low-density TJ-II discharges, hence this result in not unexpected [6]. However, more rigorous measurements over a wider density range will be performed in the near future to fully evaluate the system and these impurity temperatures.

The 100 μm slits used for these measurements together with the low plasma density of the discharge resulted in ~10^4 counts for a single line. However, somewhat higher count rates are desirable for making precise velocity measurements. The system throughput can be improved by using larger slits (200-250 μm) or by using the full fiber width (up to times 6 improvement). Moreover, some fibers, in particular those observing plasma boundary regions, could be dedicated to performing real time wavelength calibration.

Future Work

DNBI and CXRS diagnostic installation is now completed. Routine operation and exploitation will begin in the near future. Some upgrades to the diagnostic system will be made next year, e.g. optical access (although indirect) is available from a nearby tangential viewing port to permit toroidal measurements.

Acknowledgements

This work is partially financed by the Spanish *Ministerio de Educación y Ciencia*, Ref. ENE2004-04319/FTN. We are also indebted to Drs. R.E. Bell and W.L. Rowan, for consultations on several aspects raised here.

References

[1] E. Ascasíbar *et al.*, Fusion Eng. Des. **56-57** (2001) 145.

[2] K.J. McCarthy *et al.*, Rev. Sci. Instrum. **75** (2004) 3499.

[3] R. E. Bell *et al.*, Rev. Sci. Instrum. **75** (2004) 4158.

[4] D.L Hillis *et al.*, Rev. Sci. Instrum. **75** (2004) 3449.

[5] R. Balbín *et al.*, Proc. 32nd EPS Conference on Plasma Physics (Tarragona 2005), Vol. 29C D5.001.

[6] K.J. McCarthy *et al.*, Europhys. Lett. **63** (2003) 49.